

## Characterisation of the deuterium recycling at the W divertor target plates in JET during steady-state plasma conditions and ELMs

This content has been downloaded from IOPscience. Please scroll down to see the full text.

2016 Phys. Scr. 2016 014076

(<http://iopscience.iop.org/1402-4896/2016/T167/014076>)

View [the table of contents for this issue](#), or go to the [journal homepage](#) for more

Download details:

IP Address: 134.94.122.86

This content was downloaded on 15/02/2016 at 12:54

Please note that [terms and conditions apply](#).

# Characterisation of the deuterium recycling at the W divertor target plates in JET during steady-state plasma conditions and ELMs

S Brezinsek<sup>1</sup>, S Wiesen<sup>1</sup>, D Harting<sup>2</sup>, C Guillemaut<sup>3</sup>, A J Webster<sup>2</sup>,  
K Heinola<sup>2,4</sup>, A G Meigs<sup>2</sup>, M Rack<sup>1</sup>, Y Gao<sup>1</sup>, G Sergienko<sup>1</sup>, V Philipps<sup>1</sup>,  
M F Stamp<sup>2</sup>, S Jachmich<sup>5</sup> and JET Contributors<sup>6</sup>

EUROfusion Consortium, JET, Culham Science Centre, Abingdon, OX143DB, UK

<sup>1</sup>Forschungszentrum Jülich GmbH, Institut für Energie- und Klimaforschung—Plasmaphysik, 52425 Jülich, Germany

<sup>2</sup>CCFE, Culham Science Centre, Abingdon, OX14 3DB, UK

<sup>3</sup>Fonstituto de Plasmas e Fusão Nuclear, Instituto Superior Técnico, Universidade Lisboa, PT

<sup>4</sup>University of Helsinki, PO Box 64, 00014 University of Helsinki, Finland

<sup>5</sup>Laboratory for Plasmaphysics, Ecole Royale Militaire/Koninklijke Militaire School, Av de la Renaissance 30, B-1000 Brussels, Belgium

E-mail: [s.brezinsek@fz-juelich.de](mailto:s.brezinsek@fz-juelich.de)

Received 12 June 2015

Accepted for publication 18 September 2015

Published 1 February 2016



## Abstract

Experiments in the JET tokamak equipped with the ITER-like wall (ILW) revealed that the inner and outer target plate at the location of the strike points represent after one year of operation intact tungsten (W) surfaces without any beryllium (Be) surface coverage. The dynamics of near-surface retention, implantation, desorption and recycling of deuterium (D) in the divertor of plasma discharges are determined by W target plates. As the W plasma-facing components (PFCs) are not actively cooled, the surface temperature ( $T_{\text{surface}}$ ) is increasing with plasma exposure, varying the balance between these processes in addition to the impinging deuteron fluxes and energies. The dynamic behaviour on a slow time scale of seconds was quantified in a series of identical L-mode discharges (JET Pulse Number (JPN) # 81938 – 73) by intra-shot gas analysis providing the reduction of deuterium retention in W PFCs by 1/3 at a base temperature ( $T_{\text{base}}$ ) range at the outer target plate between 65 °C and 150 °C equivalent to a  $T_{\text{surface}}$  span of 150 °C and 420 °C. The associated recycling and molecular D desorption during the discharge varies only at lowest temperatures moderately, whereas desorption between discharges rises significantly with increasing  $T_{\text{base}}$ . The retention measurements represent the sum of inner and outer divertor interaction at comparable  $T_{\text{surface}}$ . The dynamic behaviour on a fast time scale of ms was studied in a series of identical H-mode discharges (JPN #83623 – 83974) and coherent edge-localized mode (ELM) averaging. High energetic ELMs of about 3 keV are impacting on the W PFCs with fluxes of  $3 \times 10^{23} \text{ D}^+ \text{ s}^{-1} \text{ m}^{-2}$  which is about four times higher than inter-ELM ion fluxes with an impact energy of about  $E_{\text{im}} = 200 \text{ eV}$ . This intra-ELM ion flux is associated with a high heat flux of about  $60 \text{ MW m}^{-2}$  to the outer target

<sup>6</sup> See the appendix of F Romanelli *et al*, Proceedings of the 25th IAEA Fusion Energy Conference 2014, Saint Petersburg, Russia



Content from this work may be used under the terms of the Creative Commons Attribution 3.0 licence. Any further distribution of this work must maintain attribution to the author(s) and the title of the work, journal citation and DOI.

plate which causes  $T_{\text{surface}}$  rise by  $\Delta T = 100$  K per ELM covering finally the range between 160 °C and 1400 °C during the flat-top phase. ELM-induced desorption from saturated near-surface implantation regions as well as deep ELM-induced deuterium implantation areas under varying baseline temperature takes place. Subsequent refuelling by intra-ELM deuteron fluxes occurs and a complex interplay between deuterium fuelling and desorption can be observed in the temporal ELM footprint of the surface temperature (IR thermography), the impinging deuteron flux (Langmuir probes), and the Balmer radiation (emission spectroscopy) as representative for the deuterium recycling flux. In contrast to JET-C, a pronounced second peak,  $\simeq 8$  ms delayed with respect to the initial ELM crash, in the  $D_\alpha$  radiation and the ion flux has been observed. The peak can be related to desorption of implanted energetic intra-ELM  $D^+$  diffusing to the W surface, and performing local recycling.

Keywords: JET-ILW, recycling, tungsten

(Some figures may appear in colour only in the online journal)

## 1. Introduction

The next step fusion test device, ITER, will employ tungsten (W) as plasma-facing material in the divertor [1] and beryllium (Be) in the main chamber. JET equipped with its ITER-like wall [2] has been used in recent years as a test-bed to study plasma-wall interaction (PWI) in this specific metallic material mix [3], as well as to explore plasma operation [4] in the carbon-free environment. Key results from the PWI studies in diverted magnetic configuration are (i) the strong reduction of long-term fuel retention [5, 6] and (ii) low material migration of Be towards the divertor [7] with respect to JET-C—JET equipped with carbon (C) walls. The inner divertor at the strike-point location is not as in JET-C in the deposition regime by the main chamber material [3, 8] which is in contradiction to initial material migration predictions made for the Be/W material mix [9]. Responsible for the difference between JET-C and JET-ILW is to a large extent the smaller primary erosion source in the main chamber inducing a lower flux of intrinsic impurities entering into the inner divertor, as well as the absence of thermally activated chemical erosion of Be [3]. Calculations with the global material migration code WallDYN confirm this physical interpretation of the Be migration with the JET-ILW [10]. The divertor PFCs, 20  $\mu\text{m}$  thick W-coating on carbon-fibre composite in the inner divertor and bulk W in the outer divertor [11], represent nearly bare W surfaces at the strike-zone areas [3]. Therefore, tungsten properties are expected to have a permanently vital impact on the divertor conditions.

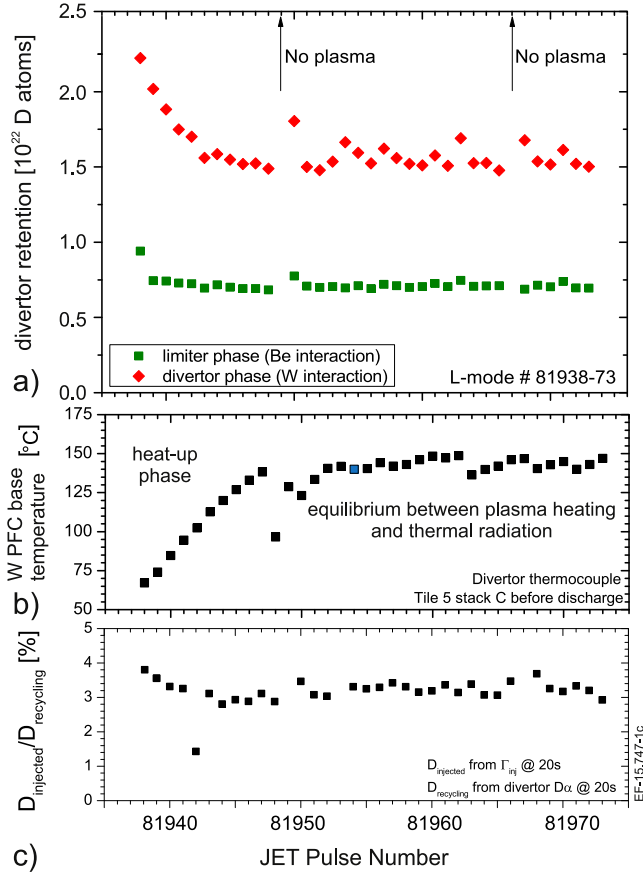
Plasma fuelling of diverted discharges in JET is predominantly determined by the fuel recycling at the target plates and to a minor extent by external gas injection of fuel ( $\simeq O(10^{-2})$ ). In the case of W the fuel reservoir is determined by the ion implantation zone, thus, indirectly by the impact energy and flux of deuterons in the case of deuterium (D) plasmas. Moreover, the D content in W depends also on the material temperature as laboratory studies demonstrated [12] as well as on the type of W PFCs, e.g. W-coating or bulk W material [13]. Due to absence of active cooling of W PFCs in JET, a large variation of surface and bulk temperature occurs in every JET discharge owing to plasma impact; a variation of the D content in W can therefore be expected. In the

following we address two experimental cases which reveal the changes of deuterium–tungsten interaction in JET on a slow time scale of seconds (L-mode conditions) and on a fast time scale of milliseconds (H-mode conditions). The latter is determined by ELM events and high energetic deuterons impinging on the target plate [14]. The interplay of retention, implantation, outgassing and recycling of D on W as a function of temperature will be analysed by a suite of diagnostics including spectroscopy, infrared thermography [15], thermocouples [16], and Langmuir probes [17].

## 2. Retention, desorption and recycling in steady-state conditions

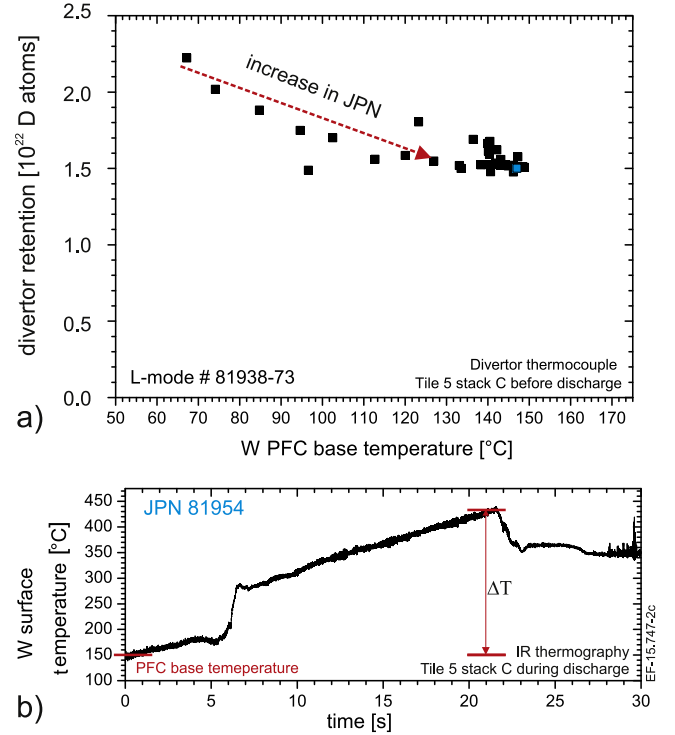
PFCs in the JET-ILW have no active cooling system but rely solely on inertial cooling to cope with the input power. The surface and bulk temperature of W divertor PFCs can vary strongly during plasma operation due to a) the steady-state power load during the discharge and b) the interplay of heating by plasma impact and radiative cooling between discharges. Variations in the surface temperature ( $T_{\text{surface}}$ ) between 65 °C at the start of an operational day and up to 1200 °C at the inner strike zone and slightly above at the outer strike zone occur depending on the plasma input power, plasma regime and duration. Here, the impact of this varying W surface and bulk conditions has been analysed in a series of identically programmed D discharges in L-mode (series I: JPN #81937 – 81973). The magnetic configuration induces interaction of the inner strike point (ISP) on the W-coated PFCs and the outer strike point (OSP) on the bulk W PFCs. Further details about the discharges executed at a plasma current of  $I_p = 2.0$  MA, a magnetic field of  $B_t = 2.4$  T, and with a total input power of  $P_{\text{tot}} = 2.5$  MW can be found in [5]. The discharge series was also used for long-term retention studies with solely turbo molecular pumping.

Figure 1(a) shows for the series of subsequent plasmas (JPN #81937 – 81973) the D retention in JET-ILW PFCs during the limiter phase, with predominately plasma interaction with Be PFCs, and during the divertor phase, with predominately plasma interaction with W PFCs. The short-term retention is determined as the time integral of the difference



**Figure 1.** (a) Fuel retention during the limiter phase (Be interaction) and the divertor phase (W and Be interaction) for a series of identical L-mode discharges (JPN #81938 – 73) [5]. (b) Variation of the base temperature of the inertially cooled bulk W PFC (tile 5) as function of the JET pulse number. (c) Variation of the contribution of injected deuterium particles to the total deuterium recycling flux, determined by  $D_{\alpha}$  in the divertor, for series JPN #81938 – 73.

between injected and exhausted deuterium particle flux in the corresponding plasma phases. As the plasma discharges of the series are set up to keep the plasma density constant, the gas injection rate is put in feed-back control. The integral short-term D retention in the limiter phase with an average ion flux to the wall of  $2 \times 10^{20} \text{ D m}^{-2} \text{ s}^{-1}$  reaches quickly after 1–2 pulses an equilibrium value. The integral short-term D retention during the divertor phase of a plasma discharge with an average ion flux to the divertor of  $3.00 \times 10^{22} \text{ D s}^{-1}$  drops from  $2.25 \times 10^{22}$  D atoms within the first ten discharges down to about  $1.50 \times 10^{22}$  D atoms. Within these first ten discharges less D is stored in the W PFCs and less injected D is required to refuel the discharge to the same plasma density. Figure 1(b) shows the increase of the bulk-W PFC  $T_{\text{base}}$  before the execution of a discharge. The data is obtained from thermocouples positioned at the bottom of the bulk W divertor module measuring the material temperature in local thermal equilibrium [11]. The first value taken before the first discharge of the day is even in full thermal equilibrium. The values for the other discharges are taken immediately before a discharge with a typical repetition rate of twenty minutes



**Figure 2.** (a) Divertor retention as function of the base temperature  $T_{\text{base}}$  inertially cooled bulk W PFC recorded before the given JET pulse number. (b) Surface temperature  $T_{\text{surface}}$  development of the bulk W PFC in L-mode discharge JPN #81954 from series JPN #81938 – 73.

between discharges. A clear increase of  $T_{\text{base}}$  from pulse to pulse within the first ten discharges can be seen. A longer break, 70 minutes before JPN #81950, leads to a substantial reduction of  $T_{\text{base}}$  as more time for radiative cooling is given. The constant discharge repetition rate provides an equilibrium between plasma heating and radiative cooling for the later series of plasmas with  $T_{\text{base}} = 145 \text{ °C}$ . Figure 1(c) provides the corresponding moderate variation in the injection rate normalized to the recycling flux in the divertor measured by the integral  $D_{\alpha}$  photon flux. The fraction of injected deuterium molecules for plasma fuelling reduces slightly from about 4% to 3% in the first few discharges and remains in the later phase constant at recycling coefficient of one with about 3.2% of fuel from  $D_2$  injection into the divertor. Recycled deuterium atoms are resulting from reflection of deuterons, from energetic charge-exchange neutrals on the W surface, and from dissociation of thermally released deuterium molecules measured by optical emission spectroscopy [18]. Note that the W PFC temperature is in this case not high enough to release directly thermal D atoms. Details of the release composition and the rovibrational population temperature of  $D_2$  are outside of this contribution.

The integral short-term D retention as function of  $T_{\text{base}}$  of the bulk W divertor PFC is depicted in figure 2(a). The reduction of the divertor retention with increasing  $T_{\text{base}}$  of the W PFCs is clearly visible until the maximum achievable temperature is reached; higher  $T_{\text{base}}$  could not be achieved with the given plasma scenario in L-mode. However, the

observed  $T_{\text{base}}$ -dependence represents only a simple parametrisation of the real behaviour with complex spatial and temporal temperature distribution during the plasma discharge. In figure 2(b) is the temporal evolution of  $T_{\text{surface}}$  depicted just before, during and shortly after a plasma discharge, thus, in the effective thermal equilibrium phase, heat-up phase during plasma impact and in the radiative cooling phase. The IR thermography shows clearly  $T_{\text{base}}$  to be equal to  $T_{\text{surface}}$  before the discharge—visualized by the measurement value at  $t = 0$  in figure 2(b)—in agreement with the thermocouple data. The maximum increase in  $T_{\text{surface}}$  during the plasma discharge, denoted as  $\Delta T$ , amounts nearly 300 K and reaches values above the first desorption peak temperature of D in W [13, 19]. The measured short-term retention is averaged over the entire divertor phase with a rising temperature and cannot resolve the precise temperature dependence of D retention in W. However, it still provides the integral information about the reduction of retention caused by implantation during deuteron impact.

Thermal diffusion into the bulk material and radiation takes place and the surface temperature drops after the plasma discharge from about 350 °C to 145 °C within the next 20 minutes prior to the next discharge. The process after the plasma discharge can be described as thermal desorption with a temperature ramp down of 10 K/min before the next plasma discharge occurs. This period contributes to the long-term outgassing and detrapping of D from low energetic trap sites in W observed before [5, 20]. It should be noted that the measured retention of D in W includes the interaction with both PFCs. These PFCs have neither the same temperature footprint nor the same W material structure. The single series measurement is insufficient to decouple the dependence of the divertor retention on the inner or outer interaction zone, and further plasma investigations with magnetic configurations employing both strike points on PFCs made with W-coated CFC are required.

### 3. Retention, desorption and recycling during ELM impact

The dynamical aspect in the deuterium–tungsten interaction is even more pronounced in H-mode plasmas with the appearance of edge-localized modes (ELMs) [21]. ELMs are short heat and energetic particle bursts leaving the confined plasma region into the scrape-off layer (SOL) and, finally, are transported to the divertor target plates. These intra-ELM particle and heat loads enhance the previously described steady-state, or inter-ELM, loads on the W PFCs. Moreover, the intra-ELM deuterons carry energies above 1 keV [14], whereas the inter-ELM deuterons have energies of about 200 eV assuming  $E_{\text{in}} = 3 \times k_B T_e + 2 \times k_B T_i$  and  $T_e = T_i = 40$  eV, thus, the ion implantation depth differs strongly for the two types of deuterons. To characterize the interaction systematically, coherent ELM-averaging analysis has been performed on a series of identical type I ELMy H-mode plasmas (series II: JPN #83623 – 83974,  $I_p = 2.0$  MA,  $B_t = 2.4$  T) with auxiliary heating  $P_{\text{aux}} = 11.0$  MW by

neutral beam injection and typical thermal energy drops of 160 kJ per ELM. ELMs appeared in the six seconds long flat-top phase of the discharge with frequency about 30 Hz. Plasma fuelling was carried out with gas injection of  $1.0 \times 10^{22}$  D s<sup>-1</sup> into the divertor in feed forward with active divertor cryogenic pumping (cf case e in [5]). The magnetic configuration in this plasma series II is identical to the previously described L-mode case with the ISP positioned on the W-coated CFC and the OSP on the bulk W divertor target plate. IR thermography observing the OSP with high temporal resolution of a few s [15, 21] provides a peak heat load of about 60 MW m<sup>-2</sup> during an ELM impact. The peak surface temperature of the W divertor at the OSP (tile 5, stack C) exceeds 1400 °C at the end of the flat-top phase starting from a base level temperature of about 160 °C as depicted in figure 3(a) for a representative discharge from series II. Figure 3(a) shows further the temperature rise in the neighbored, thermally isolated bulk W segment (tile 5, stack D) located in the SOL. ELMs appear as individual fast temperature bursts of a few ms duration with incremental increase of about 120 K on top of the baseline temperature rise. This ELM-induced increase is quantified in figure 3(b) which shows the temporal and spatial  $T_{\text{surface}}$  evolution of a coherent ELM of series II. The coherent-averaged ELM consists of more than 1600 individual ELM footprints recorded in the last 2.0 s of the flat-top phase in series 2 discharges corresponding to surface temperatures above  $\approx 800$  °C where the temporal ELM footprint appears self-similar. In contrast, the temporal evolution of the ELM footprint varies dramatically in the temperature range between 300 °C and 800 °C, as depicted in figure 3(c).

Figure 3(c) shows five 300 ms long lasting snapshots of the W peak surface temperature evolution at the OSP (tile 5, stack C) and the SOL (tile 5, stack D) distributed over the H-mode phase of a characteristic discharge (JPN #83660) of series II. The temporal ELM signature measured at stack D during the first second of the H-mode flat-top phase (JPN #83660) are obtained at the lowest accessible surface temperature domain ( $T_{\text{surface}} = 300$  °C  $\leq$  450 °C). These footprints show the shortest ELM duration in this characteristic discharge—similar to ELM signatures found previously in JET-C [21]. The same early ELMs of discharge JPN #83660 reaching the location of the OSP are obtained already at  $T_{\text{surface}} > 500$  °C and show a completely different temporal ELM behaviour. At first the typical temperature rise occurs when the heat load arrives at the target, but then a pronounced temperature drop after the end of the ELM crash can be observed. The drop is caused by local plasma cooling due to D<sub>2</sub> outgassing which reduces the inter-ELM heat load reaching the target plate before the next ELM arrives. This outgassing and cooling is spatially restricted in radial direction and its strength depends on the fuel content in the W PFC near surface and the surface temperature. The desorption reduces with rising  $T_{\text{surface}}$  under constant ELM impact because less D is stored in the W PFC surface at higher  $T_{\text{surface}}$ , as shown in the L-mode case. This second desorption process also takes place at the neighbored stack D at the



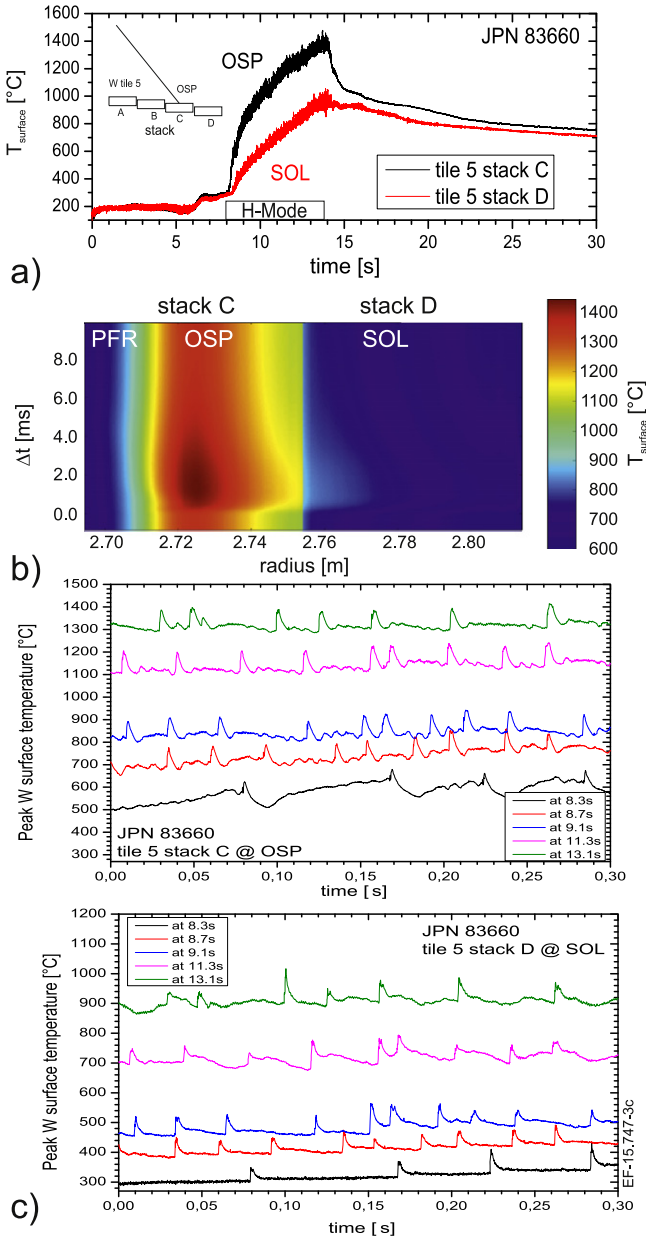


**Figure 3.** (a) Temporal evolution of  $T_{\text{surf}}$  at the outer strike point (OSP) (tile 5, stack C) and the scrape-off layer (SOL) (tile 5, stack D) measured by IR thermography for discharge JPN #83660. (b) Spatial and temporal footprint of a coherent-averaged ELM at the outer target plate deduced from a series of identical H-mode discharges (series II: JPN #83623 – 83974). The private flux region (PFR), OSP and the SOL are labelled. (c) Five 300 ms snapshots of the  $T_{\text{surface}}$  evolution during the H-mode phase (#JPN83660) with typically ten ELM impacts. Variation of the temporal ELM footprint with  $T_{\text{surface}}$  rise on tile 5 at the OSP (stack C) and in the SOL (stack D).

same local  $T_{\text{surface}}$ , but is temporally delayed with respect to the interaction at the OSP positioned on stack C.

This temperature span is similar on the W PFCs at the ISP, thus, the release occurs at both divertor legs. The  $D_2$  desorption at the ISP is even sufficient to reach detachment after the ELM crash. Such post ELM-induced detachment by

outgassing is comparable to observations in JET-C on deuterium-rich a-C:D layers under impact of ELMs with thermal energy drops of 500 kJ or more [22] reaching  $T_{\text{surface}}$  of 1600°C. However, in the JET-ILW case there is not enough implanted D in the near W surface at the OSP to achieve post-ELM crash detachment.

Further comparison with JET-C also showed a new phenomena associated with the temporal ELM footprint with the W PFCs. Figure 4 shows from top to bottom the coherent ELM-averaging for the total impinging ion flux to the outer divertor, the Balmer- $\alpha$  photon flux for the particle recycling, the *BeII* photon flux for the impinging intrinsic impurities, and the *WI* photon flux for the sputtered W at the target plate. The impinging ion flux and the recycling flux show a pronounced second peak about 8 ms after the initial ELM crash which has not been observed in JET-C. In contrast the impinging Be ion flux and W sputtering flux show no second peak which indicates that a) this peak is not related to ions arriving from the pedestal region and b) the impact energy of the ions is below the sputtering threshold for W by Be or D. The coherent appearance of impinging deuterons and neutral atom radiation suggests that the origin of the secondary peak is related to temporary appearance of local recycling at the target plate. Thermal release of  $D_2$  and subsequent dissociation and ionisation can provide the low energetic deuteron flux which has been observed. The required local deuterium source is most probably related to the implanted energetic intra-ELM deuterons diffusing to the W surface. The time to diffuse will depend on the implantation depth and the temperature of the W plate and can therefore explain the observed difference in the time span between the first and second peak in the ion and recycling flux. Details about the longer lasting post-ELM oscillations over the subsequent forty milliseconds can be found in [23, 24]. Their origin can be attributed to the vertical plasma positioning at JET.

#### 4. Summary and conclusion

Experiments at JET-ILW have been carried out and revealed that the inner and outer target plate at the location of the strike points represents clean W surfaces without any Be surface coverage. The dynamics of near-surface retention, implantation, outgassing and recycling of deuterium on W are fully developed during plasma operation in JET-ILW. The balance between these processes is varying as all W PFCs, the W-coated CFC as well as the bulk W, are not actively cooled and the surface temperature  $T_{\text{surface}}$  is increasing with plasma loading. The dynamic behaviour on a slow time scale of seconds was investigated in a series of identical L-mode discharges (JPN #81938 – 73) by intra-shot gas analysis providing the reduction of the short-term fuel retention in W PFCs by 1/3 at a base temperature  $T_{\text{base}}$  range between 65 °C and 150 °C equivalent to a  $T_{\text{surface}}$  span of 150 °C and 420 °C. The  $T_{\text{surface}}$  reaches also the first deuterium desorption peak

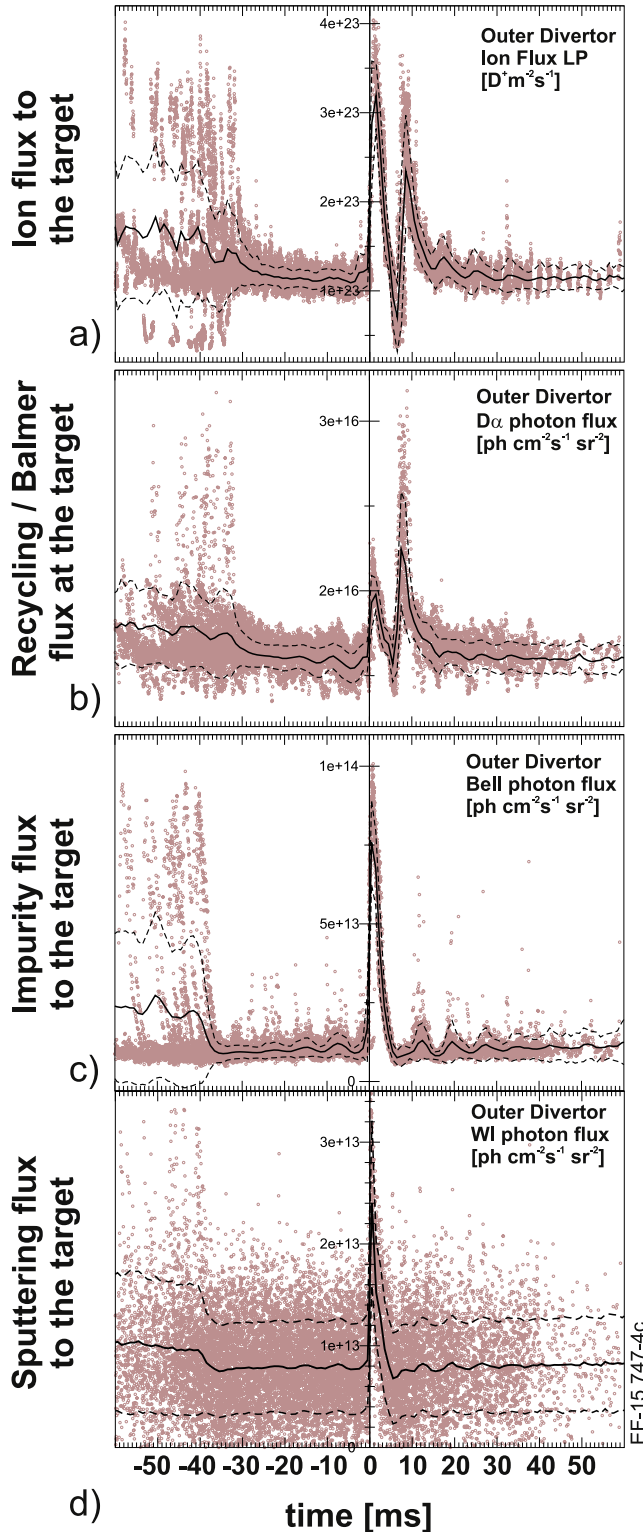


**Figure 4.** Coherent ELM averaging of H-mode discharges (series II: JPN #83623 – 83974). The time period 50 ms before and after the ELM crash are shown for the magnetic low-field side. (a) Total impinging ion flux measured by Langmuir Probes, (b) total  $D_{\alpha}$  photon flux as marker for recycling, (c) photon flux resulting from impinging Be ions (*Bell* at 527.1 nm), and (d) photon flux of sputtered W atoms from the bulk-W divertor PFCs (*WI* at 400.9 nm).

found by thermal desorption spectroscopy JET W-coated PFCs after extraction [19].

In a second discharge series (H-mode: JPN #83623 – 83974), the dynamic behaviour on the time scale of ms due to ELMs interacting with the W target plate was studied. ELM-induced desorption from saturated near-surface and implantation W regions as well as deep ELM-induced deuterium implantation under varying baseline temperature takes place. Subsequent refuelling by intra-ELM deuteron fluxes occurs and a complex interplay between deuterium refuelling and desorption can be observed in the temporal ELM footprint of the surface temperature, impinging deuteron flux, and deuterium recycling flux. In contrast to JET-C, a pronounced second peak,  $\approx 8$  ms delayed with respect to the initial ELM crash, in the  $D_{\alpha}$  radiation and the ion flux has been observed and related low energetic neutrals and deuterons performing local recycling. The required deuterium source is most likely related to the implanted energetic intra-ELM deuterons diffusing to the W surface and are thermally desorbed away.

It is a fair question if the situation in JET with ILW is comparable to ASDEX Upgrade (AUG) in the configuration of 1998/1999—low Z main chamber (graphite) and high Z divertor (tungsten) PFCs ([25] and references within)—and why this dynamic recycling and retention behaviour in W has not been identified before. Though there is an interplay of low Z and high Z in both cases the situation is in fact different between AUG and JET-ILW due to the higher impurity concentration of low Z in AUG at that time. The first wall erosion due to chemical and physical sputtering of graphite PFCs induced C concentrations above 2% in the plasma and influxes of C to the outer divertor to more than 1%. As a consequence, the outer divertor of AUG was covered by a protective C layer due to C deposition on W and C implantation in W. Moreover, C migration from the main chamber into the inner divertor took place and caused massive C deposition and the formation of thick a-C:D layers with high deuterium content on the W PFCs [25]. De facto the first W divertor in AUG was masked by C and therefore the local dynamics during ELM interaction were determined by C properties and not by W like in JET-ILW. Indeed, this makes the difference as the fuel (D) content in a-C:D layers is significantly higher than D implanted in bulk W. The D reservoir was almost infinite in the AUG case for typical ELM energy drops in the order of 20 kJ. In contrast, JET with the ILW has a very low impurity concentration and both divertor legs represent net W erosion zones [3], and are, as such, prone to the dynamics in the deuterium content and recycling presented in this contribution.

## Acknowledgments

This work has been carried out within the framework of the EUROfusion Consortium and has received funding from the

Euratom research and training programme 2014–2018 under grant agreement No. 633053. The views and opinions expressed herein do not necessarily reflect those of the European Commission.

## References

- [1] Hirai T *et al* 2015 *J. Nucl. Mater.* **463** 1248
- [2] Matthews G F *et al* 2013 *J. Nucl. Mater.* **438** S2
- [3] Brezinsek S *et al* 2015 *J. Nucl. Mater.* **463** 11
- [4] Joffrin E *et al* 2014 *Nucl. Fusion* **54** 013011
- [5] Brezinsek S *et al* 2013 *Nucl. Fusion* **53** 083023
- [6] Heinola K *et al* 2015 *J. Nucl. Mater.* **463** 961
- [7] Brezinsek S *et al* 2015 *Nucl. Fusion* **55** 063021
- [8] Mayer M *et al* 2016 *Phys. Scr.* **2016** 014051
- [9] Roth J *et al* 2009 *J. Nucl. Mater.* **390–3** 1
- [10] Schmid K *et al* 2015 *J. Nucl. Mater.* **463** 11
- [11] Mertens Ph *et al* 2011 *Phys. Scr.* T **145** 014002
- [12] Roszell J P *et al* 2012 *J. Nucl. Mater.* **429** 48
- [13] Sugiyama K *et al* 2014 *Phys. Scr.* T **159** 014043
- [14] Guillemaut Ch *et al* 2016 *Phys. Scr.* **2016** 014005
- [15] Balboa I *et al* 2012 *Rev. Sc. Instr.* **83** 10D530
- [16] Mertens Ph *et al* 2009 *J. Nucl. Mater.* **390–391** 967
- [17] Guillemaut Ch *et al* 2015 *Plasma Phys. Control. Fusion* **57** 085006
- [18] Sergienko G *et al* 2013 *J. Nucl. Mater.* **438** S1100
- [19] Likonen J *et al* 2016 *Phys. Scr.* **2016** 014074
- [20] Bission R, Markelj S, Mourey O, Ghiorghiu F, Achkasov K, Layet J-M, Roubin P, Cartry G, Grisolia C and Angot T 2015 *J. Nucl. Mater.* **476** 432–8
- [21] Eich T *et al* 2013 *J. Nucl. Mater.* **438** S72
- [22] Huber A *et al* 2011 *J. Nucl. Mater.* **415** S821
- [23] Webster A J *et al* 2014 *Phys. Plasmas* **21** 112502
- [24] Webster A J *et al* 2015 *Phys. Plasmas* **22** 085201
- [25] Neu R *et al* 2003 *Fusion Sci. Technol.* **44** 692